Investigation of anisotropy in nonsaturated and heterogeneous carbonate series using crosshole acoustic techniques

Dawin Baden, Pierre Henry, Ginette Saracco, Lionel Marié, Yves Guglielmi

Investigation of anisotropy in non-saturated and heterogeneous carbonate series using crosshole acoustic technics

Dawin Baden, Pierre Henry, Ginette Saracco, and Lionel Marié, Aix-Marseille Université, CNRS, CEREGE, IRD; Yves Guglielmi, Lawrence Berkeley National Laboratory*

Physical properties of carbonate rocks cannot be fully captured from laboratory-sized samples. Indeed, heterogeneous facies distribution and/or diagenetic alterations may lead to significant variations in petrophysical properties within few meters. In carbonates, diagenetic transformations are tightly related to nature of fluids flowing through the formations, e.g. via fractures network. Consequently, reservoir properties may have patchy distribution, and may not be correlatable (e.g. using facies distribution or wells-logs correlations) within few meters. Our works aim at characterizing carbonates anisotropy at different scales, and are subject of two presentations at SEG's 87th Annual Meeting. This abstract deals with the first part of our approach, that's to say characterizing impact of diagenetic alteration on reservoir properties and seismic anisotropy, from meter to multi-meter scale. Crosshole acoustic-survey has been carried out using ultrasonic frequencies (50kHz), and vertical-resolution of 10cm. The main conclusions are: (1) multi-meter crosshole surveys, enable measuring elastic properties of both matrix, and fractured-matrix. Wave velocities measured at multi-meter scale are comparable to that from laboratory measurements, and this analogy is attributed to poor likelihood of finding dense fractures-sets –which would drastically change elastic moduli– at reduced scale. (2) Weak anisotropy is detected, varying between +10% (slow axis perpendicular to strata) and –2% (slow axis parallel to strata), and likely results from combination of matrix anisotropy (mineral orientation and pore geometry) and fractures effects. (3) In heterogeneous layered formations, variation of mean velocity with source and receivers locations significantly impact anisotropy parameters estimated by curve fitting. One should be aware of this potential bias, while interpreting crosshole surveys with sparse data, especially in carbonate formations.

Introduction:

This study is consecutive to a series of published works aiming at characterizing both reservoir and elastic properties of Lower Cretaceous limestone from the Urgonian platform of Provence (SE, France). References describing the characteristics of this platform in terms of facies, and biostratigraphy are available e.g. (Leonide et al. 2012). These microporous bioclastic limestones are analogues of different hydrocarbon reservoirs in Middle East, e.g. Kharaib and Shuaiba formations (Borgomano et al. 2013). In addition, several published databases document coupled porosity, and elastic waves velocities measurements from the Urgonian platform (Fournier and Borgomano 2009; Fournier et al. 2011; Fournier et al. 2014; Borgomano et al. 2013). In these works, the authors used conventional laboratory approach, i.e. velocity measurements carried out on 1" to 1.5" mini-cores, under effective stress; and they discussed "*effective media theory*", and the concept of "*pore aspect ratio*" extensively. Nevertheless, a known limitation of these approaches is the implicit assumption of medium's isotropy. Despite this assumption is generally true at the plug scale, it is rarely the case at larger scale. Carbonate rocks are often fractured and may have either "*facies-related"* or *"patchy"* porosity distribution that may lead to seismic anisotropy.

The works presented here focus on the impact of up-scaling onto elastic properties of carbonates rocks. Crosshole ultrasonic measurements have been carried out *in situ*, and the results are compared to published works, and to our multi-scale laboratory approach (cf. our second presentation).

Geological context:

The study took place in SE France, in an underground facility, namely LSBB (Low Noise Underground Laboratory). The LSBB is a network of sub-horizontal galleries dug in thick Barremian bioclastic limestone, within the vadose zone of *"Fontaine de Vaucluse"* aquifer system. The study site was located in the GAS-gallery (Figure 1), ~250m below the surface topography, which enables to set up experiments in subsurface conditions, at least in terms of hydrostatic stress, *Guglielmi et al.*, [2015] estimated the main stress to 6MPa. The gallery gives direct access to the 30° southward-dipping layers, and five vertical fully-cored boreholes (~20m deep) named P1 to P5 were drilled in 2009, and were studied as part of previous works (Jeanne 2012; Jeanne, Guglielmi, and Cappa 2013; Jeanne, Guglielmi, and Cappa 2012; Jeanne et al. 2012).

The geological background over the studied interval is summarized in Figure 2. The south-dipping layers intersected by the boreholes are inner-platform facies i.e. low to moderate energy, muddy or peloidal carbonate sands with abundant rudists. The cores' analysis emphasized two main facies types: (1) calcarenites (grainstone to rudstone), and (2) calcilutites (wackestone to packestone). Since the reservoir properties are not related to facies, but instead to diagenesis (Léonide et al. 2014), we do not describe them any further in this abstract. The studied interval can be divided in three mechanical units: two are densely fractured (from 1 to 6m, and from 14 to 21m), and one is moderately fractured (from 6 to 14m). The formation is affected by two sets of sub-vertical fractures (dip ~80°), and oriented N30 and N120. The fractures density is controlled by

both porosity and the fault zone nearness (Jeanne, Guglielmi, and Cappa 2012; Jeanne, Guglielmi, and Cappa 2013). The open-fractures sets are located mainly in area with gradual porosity changes close to the calcilutites. Under pressure-solution conditions, the calcilutites may have produced carbonate rich fluids (cf. stylolites) that migrated and precipitated nearby, occluding some of the fractures and decreasing locally the overall porosity of the porous layer.

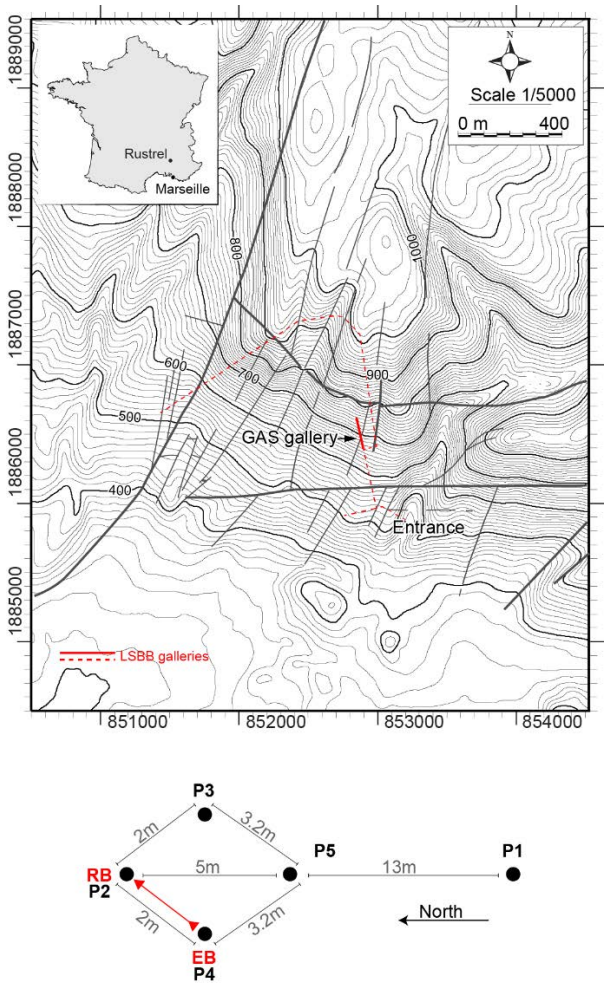

Figure 1. Localization GAS-gallery in the LSBB, and disposition of the boreholes.

Material and methods:

The acoustic logging has been carried out between P4 (Emission Borehole), and P2 (Reception Borehole) located two meters apart, along azimuth N20°. The study was conducted from 1 to 14.5m depth. The acquisition was divided into sections for technical reasons, each section is 1.5m high, and the spacing of the sensor array was 10cm. For each section 256 full-waveforms acoustic signals were recorded. The P- and S-waves travel times were manually picked and were processed, section by section, according to raypaths angles. This approach emphasized angular dependency of elastic wave velocities, and a correlation with beddings. Data were investigated using a model of anisotropic media, the transverse isotropy (TI). TI media have same properties in one plane (e.g. the x-y plane) and different properties in direction normal to this symmetry plane (e.g. z-axis). If the z-axis is the vertical axis, then the material is a Vertical Transversely Isotropic medium (VTI). For such material, the stiffness tensor (C_{IJ}) written in Voigt's notation, requires only five independent components to fully describe its elasticity.

$$C_{IJ} = \begin{pmatrix} c_{11} & c_{12} & c_{13} & & & \\ c_{12} & c_{11} & c_{13} & & & \\ c_{13} & c_{13} & c_{33} & & & \\ & & & c_{44} & & \\ & & & & c_{44} & \\ & & & & & c_{66} \end{pmatrix}, \quad c_{66} = \frac{c_{11} - c_{12}}{2} \qquad (1)$$

After equation (2), the components of C_{IJ} can be obtained from 5 velocity measurements (Mavko, Mukerji, and Dvorkin 2009).

$$\begin{aligned} c_{11} &= \rho Vp^2_{(90°)} \\ c_{33} &= \rho Vp^2_{(0°)} \\ c_{44} &= \rho Vsh^2_{(0°)} \\ c_{66} &= \rho Vsh^2_{(90°)} \\ c_{13} &= -c_{44} + \left(\begin{array}{l} 4\rho^2 Vp^4_{(45°)} - 2\rho Vp^2_{(45)} \\ \times (c_{11} + c_{33} + 2c_{44}) \\ + (c_{11} + c_{44})(c_{33} + c_{44}) \end{array} \right)^{1/2} \end{aligned} \qquad (2)$$

The model of VTI media enables to compute phase velocities for quasi-longitudinal (Vp), quasi-shear (Vsv), and pure-shear (Vsh) modes, see equation below.

$$\begin{aligned} Vp(\theta) &= \left(c_{11}\sin^2\theta + c_{33}\cos^2\theta + c_{44} + \sqrt{M} \right)^{1/2} (2\rho)^{-1/2} \\ Vsv(\theta) &= \left(c_{11}\sin^2\theta + c_{33}\cos^2\theta + c_{44} - \sqrt{M} \right)^{1/2} (2\rho)^{-1/2} \\ Vsh(\theta) &= \left(\frac{c_{66}\sin^2\theta + c_{44}\cos^2\theta}{\rho} \right)^{1/2} \\ M &= \left[(c_{11} - c_{44})\sin^2\theta - (c_{33} - c_{44})\cos^2\theta \right]^2 \\ &\quad + (c_{13} + c_{44})^2 \sin^2 2\theta \end{aligned} \qquad (3)$$

Where ρ is the density, and θ is the phase's angle.

Finally, the phase velocities were converted into group velocities for direct comparison with the field data, and the stiffness components were compared to values documented in literature on Urgonian limestones.

Results and Discussion:

The velocity distribution is consistent with porosity variations within the studied area (Figure 2), and the dipping of the layers (~30°), is well figured. The highest velocities [~6.5 – 6.3km/s] are between 1 and 5.5m depth, which is a low porous interval.

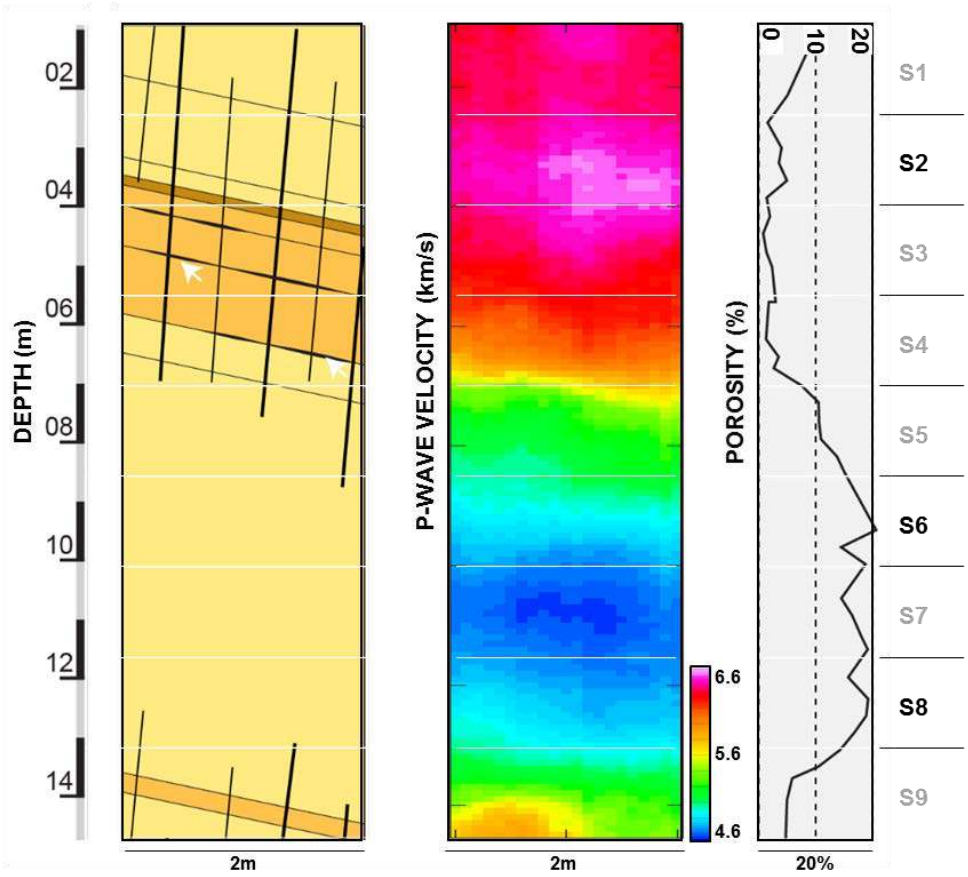

Figure 2. *Tomography of inter-borehole space, put in perspective with a schematic view of the geology, and the porosity (adapted from* Jeanne et al. (2012)*. The tomography of P-wave velocity was computed using the eikonal equation (D. Baden et al. 2017, submitted).*

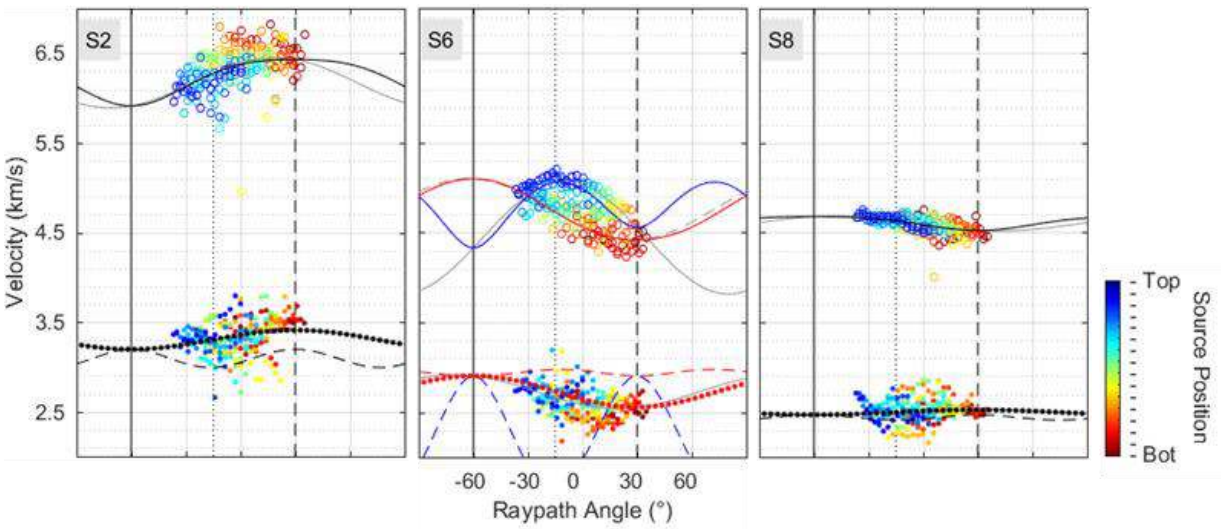

Figure 3. Velocity models computed using the computed stiffness coefficients. The P- and S-wave velocities are figured by open circles and dots, respectively. The solid, the dotted and the dashed models stand for: Vp, Vsh, and Vsv, respectively. The cosine models (grey) are also plotted for comparison but are not discussed in this abstract.

The lowest velocities [~4.6–4.8km/s] are from 9 to 13m, where porosity reaches up to 20%. Two intervals with intermediate velocities ~5.2km/s located between ~7 and 8m and from 13 to 14.5m, show porosity variation. Although the tomography have fair consistency with the porosity, yet the anisotropy visible in data (e.g. Figure 3) seems smoothed by such the process.

One can see that transverse isotropy approximation was relevant in this study, since phase velocity models are consistent with experimental data (Figure 3). Taking the example of S2, which is a high velocity interval with P-wave velocity anisotropy ~10%. The direction of maximum velocity is 30° which means it follows the stratification. One would expect having slow axis normal to beddings, but in our context, fractures-sets are normal to layers, since they are dry the reduction of elastic modulus is maximum perpendicular to the their orientation (Hudson 1980; Hudson 1981; Rüger 1997; Guéguen and Sarout 2009; Tsvankin 1997). So that, the anisotropy observed in S2 could be explained either by stress relief (and thus opening of fractures-sets), or presence of stylolithes (Baud et al. 2015).

The second example, S8, shows despite detected anisotropy is relatively small, the value is reliable. Data from this interval showed great consistency for successive shots, and anisotropy measurements made on the matrix *(cf. our 2nd presentation at SEG's 87th Annual Meeting)*, showed that the higher the intercrystalline porosity (i.e. between micrite crystals), the more the matrix was anisotropic. Moreover, this interval have few macroscopic fractures, which leaves porosity fabric and mineral orientation as the most likely explanations for this anisotropy.

The particularity of S6, which is our last example, lies into the fact that there is an obvious influence of the source location on the anisotropy. This interval has increasing porosity values bottomward, plus, it is an area were fractures attenuate as they reach the porous layer. The change in the anisotropy simply show that two anisotropies (matrix and fractures) are convoluted there.

In Table 1, our results are compared to other works conducted on the same carbonates, at seismic-scale (≤180m) in Bereš et al. (2013), at field-scale (≤13.5m) in this study, and at laboratory-scale (=2.54cm) in Fournier et al. (2014).

Table 1. C_{IJ} components for Urgonian limestones (Baden et al., *@submitted article*).

($\times 10^9$)	*Bereš et al.*, [2013]	*Baden et al., (submitted)*	*Fournier et al.*, [2014]
C_{11}	44,9 - 36,9	108,0 – 41,4	110,4 - 26,8
C_{13}	19,7 - 18,3	52,5 – 6,1	52,7 - 9,2
C_{33}	69,2 - 65,9	99,6 – 43,4	C_{11}
C_{44}	19,7 - 18,3	30,3 –- 13,7	34 - 7,9
C_{66}	15,4 - 14,8	30,4 – 12,5	C_{44}

The smaller the sample the higher the coefficients variability, this is explained, by averaging effect of the scale. Indeed, different factors, i.e. facies, grains sorting, and diagenesis cause heterogeneity in carbonate rocks. Hence the smaller the samples the greater the probability of sampling particular features. Accordingly, elastic properties are averaged with the increasing scale. Interestingly, even if major fractures are present in the sections, our stiffness coefficients are closer to laboratory values than seismic-scale ones. This suggests that at meter-scale, fractures start to be sampled but do not dominate the signal, which enables to capture both signatures of the matrix and the fractures. In addition, the faults present in the LSBB area (Jeanne 2012), and which did not affect our measurements (no fault between the tested boreholes), but which were unavoidably measured by *Bereš et al.*, [2013], may have played a role even bigger in lowering the velocities than fractures-sets alone. For example Al-Harrasi et al. (2011) related the anisotropy in the Natih carbonate reservoir (Oman) the rock type and proximity to major faults. So that, the coefficients presented in this study may be representative of the rock matrix and of the fractured rock, whereas at seismic-scale, major faults may obliterate the effects of the matrix, hence, seismic-scale coefficients may be more representative of faulted rock mass.

Conclusion:

A crosshole acoustic-survey has been carried-out using ultrasonic frequencies (50kHz), and with vertical-resolution of 10cm. This works were conducted in order to characterize, in situ, a microporous carbonate series from meter to decameter scale. The main conclusions can be summarized as follow:

(1) Crosshole ultrasonic surveys enable measuring elastic properties of both matrix, and fractured-matrix. The wave velocities measured at multi-meter scale are comparable to that from conventional laboratory measurements. This similarity can be attributed to the poor likelihood of finding multiple fractures as the dimensions of investigated area decreases.

(2) In most cases, a weak anisotropy is detected, varying between +10% (slow axis perpendicular to strata) and –2% (slow axis parallel to strata) and likely results from a combination of matrix anisotropy (mineral orientation and pore geometry) and fractures effects.

(3) In heterogeneous layered formations, variation of mean velocity with source and receivers locations significantly impact anisotropy parameter estimated by curve fitting. One should be aware of this potential bias, while interpreting crosshole surveys with sparse data, especially in carbonate formations.

Acknowledgements:

This works were supported by two Research programs: H–CUBE project (ANR-12-SEED-0006), D. Baden's PhD grant; and ALBION-HPMSCa project, funded by TOTAL .

EDITED REFERENCES

Note: This reference list is a copyedited version of the reference list submitted by the author. Reference lists for the 2017 SEG Technical Program Expanded Abstracts have been copyedited so that references provided with the online metadata for each paper will achieve a high degree of linking to cited sources that appear on the Web.

REFERENCES

Al-Harrasi, O. H., A. Al-Anboori, A. Wüstefeld, and J.-M. Kendall, 2011, Seismic anisotropy in a hydrocarbon field estimated from microseismic data: Geophysical Prospecting, **59**, 227–243, http://doi.org/10.1111/j.1365-2478.2010.00915.x.

Baud, P., A. Rolland, M. Heap, T. Xu, M. Nicolé, T. Ferrand, T. Reuschlé, R. Toussaint, and N. Conil, 2015, Impact of stylolites on the mechanical strength of limestone: Tectonophysics, **690**, 4–20, http://doi.org/10.1016/j.tecto.2016.03.004.

Bereš, J., H. Zeyen, G. Sénéchal, D. Rousset, and S. Gaffet, 2013, Seismic anisotropy analysis at the Low-Noise Underground Laboratory (LSBB) of Rustrel (France): Journal of Applied Geophysics, **94**, 59–71, http://doi.org/10.1016/j.jappgeo.2013.04.008.

Borgomano, J., J.-P. Masse, M. Fenerci-Masse, and F. Fournier, 2013, Petrophysics of Lower Cretaceous Platform Carbonate Outcrops in Provence (SE France): Implications for carbonate reservoir characterisation: Journal of Petroleum Geology, **36**, 5–42, http://doi.org/10.1111/jpg.12540.

Fournier, F., and J. Borgomano, 2009, Critical porosity and elastic properties of microporous mixed carbonate-siliciclastic rocks: Geophysics, **74**, no. 2, E93–E109, http://doi.org/10.1190/1.3043727.

Fournier, F., P. Leonide, K. Biscarrat, A. Gallois, J. Borgomano, and A. Foubert, 2011, Elastic properties of microporous cemented grainstones: Geophysics, **76**, no. 6, E211–E226, http://doi.org/10.1190/geo2011-0047.1.

Fournier, F., P. Léonide, L. Kleipool, R. Toullec, J. J. G. Reijmer, J. Borgomano, T. Klootwijk, and J. Van Der Molen, 2014, Pore space evolution and elastic properties of platform carbonates (Urgonian Limestone, Barremian-Aptian, SE France): Sedimentary Geology, **308**, 1–17, http://doi.org/10.1016/j.sedgeo.2014.04.008.

Guéguen, Y., and J. Sarout, 2009, Crack-induced anisotropy in crustal rocks: Predicted dry and fluid-saturated Thomsen's parameters: Physics of the Earth and Planetary Interiors, **172**, 116–124, http://doi.org/10.1016/j.pepi.2008.05.020.

Guglielmi, Y., F. Cappa, J.-P. Avouac, P. Henry, and D. Elsworth, 2015, Seismicity triggered by fluid injection-induced aseismic slip: Science, **348**, 1224–1226, http://doi.org/10.1126/science.aab0476.

Hudson, J. A., 1980, Overall properties of a cracked solid: *Mathematical Proceedings of the Cambridge Philosophical Society*, **88**, 371–384, http://doi.org/10.1017/S0305004100057674.

Hudson, J. A., 1981, Wave speeds and attenuation of elastic waves in material containing cracks: Geophysical Journal of the Royal Astronomical Society, **64**, 133–150, http://doi.org/10.1111/j.1365-246X.1981.tb02662.x.

Jeanne, P., 2012, Architectural, petrophysical and hydromechanical properties of fault zones in fractured-porous rocks: Compared studies of a moderate and a mature fault zones (France): Aix-Marseille Université.

Jeanne, P., Y. Guglielmi, and F. Cappa, 2012, Multiscale seismic signature of a small fault zone in a carbonate reservoir: Relationships between VP imaging, fault zone architecture and cohesion: Tectonophysics, **554–557**, 185–201, http://doi.org/10.1016/j.tecto.2012.05.012.

Jeanne, P., Y. Guglielmi, and F. Cappa, 2013, Dissimilar properties within a carbonate-reservoir's small fault zone, and their impact on the pressurization and leakage associated with CO_2 injection: Journal of Structural Geology, **47**, 25–35, http://doi.org/10.1016/j.jsg.2012.10.010.

Jeanne, P., Y. Guglielmi, J. Lamarche, F. Cappa, and L. Marié, 2012, Architectural characteristics and petrophysical properties evolution of a strike-slip fault zone in a fractured porous carbonate reservoir: *Journal of Structural Geology,* **44**, 93–109, http://doi.org/10.1016/j.jsg.2012.08.016.

Leonide, P., J. Borgomano, J.-P. Masse, and S. Doublet, 2012, Relation between stratigraphic architecture and multi-scale heterogeneities in carbonate platforms: The Barremian-lower Aptian of the Monts de Vaucluse, SE France: *Sedimentary Geology,* **265–266**, 87–109, http://doi.org/10.1016/j.sedgeo.2012.03.019.

Léonide, P., F. Fournier, J. J. G. Reijmer, H. Vonhof, J. Borgomano, J. Dijk, M. Rosenthal, M. van Goethem, J. Cochard, and K. Meulenaars, 2014, Diagenetic patterns and pore space distribution along a platform to outer-shelf transect (Urgonian Limestone, Barremian-Aptian, SE France): *Sedimentary Geology,* **306**, 1–23, http://doi.org/10.1016/j.sedgeo.2014.03.001.

Mavko, G., T. Mukerji, and J. Dvorkin, 2009, *The rock physics handbook*, 2nd ed.: Cambridge University Press.

Rüger, A., 1997, P-wave reflection coefficients for transversely isotropic media with vertical and horizontal axis of symmetry: *Geophysics,* **62**, 713–722, http://doi.org/10.1190/1.1444181.

Tsvankin, I., 1997, Reflection moveout and parameter estimation for horizontal transverse isotropy: *Geophysics,* **62**, 614–629, http://doi.org/10.1190/1.1444170.